

Minerva Access is the Institutional Repository of The University of Melbourne

Author/s:

Guntari, SN;Khin, ACH;Wong, EHH;Goh, TK;Blencowe, A;Caruso, F;Qiao, GG

Title:

(Super)hydrophobic and multilayered amphiphilic films prepared by continuous assembly of polymers

Date:

2013-11-06

Citation:

Guntari, S. N., Khin, A. C. H., Wong, E. H. H., Goh, T. K., Blencowe, A., Caruso, F. & Qiao, G. G. (2013). (Super)hydrophobic and multilayered amphiphilic films prepared by continuous assembly of polymers. *Advanced Functional Materials*, 23 (41), pp.5159-5166. <https://doi.org/10.1002/adfm.201300768>.

Persistent Link:

<https://hdl.handle.net/11343/123309>

(Super)hydrophobic and Multilayered Amphiphilic Films Prepared by Continuous Assembly of Polymers

By *Stefanie N. Guntari, Aaron C. H. Khin, Edgar H. H. Wong, Tor K. Goh, Anton Blencowe, Frank Caruso,* and Greg G. Qiao**

[*] Prof. G. G. Qiao, Prof. F. Caruso
Department of Chemical and Biomolecular Engineering
The University of Melbourne
Victoria 3010 (Australia)
E-mail: gregghq@unimelb.edu.au, fcaruso@unimelb.edu.au

Keywords: nanotechnology, ROMP, amphiphilic films, superhydrophobic surface.

Abstract

The continuous assembly of polymers (CAP) is used to fabricate tailored nanocoatings on a wide variety of substrates. Ring opening metathesis polymerization (ROMP) is used to mediate the CAP process (CAP_{ROMP}) to assemble specifically designed macromolecules into nanoengineered cross-linked films. Different films composed of single or multiple macromolecules are used to tune the surface wetting characteristics on various planar substrates, including porous substrates such as filter paper and cotton, and non-porous substrates such as aluminium foil, and glass. By judicious selection of the macromolecules, these substrates, which are hydrophilic in nature, can be rendered (super)hydrophobic. The robustness of the ROMP catalysts and the reinitiation ability of the CAP_{ROMP} approach allow for the production of layered multicomponent amphiphilic films with on-demand switchable wettability. Such functional nanocoatings can be potentially applied as advanced materials as

self-cleaning surfaces, waterproof woven fabrics, and the next generation of microelectronic devices.

1. Introduction

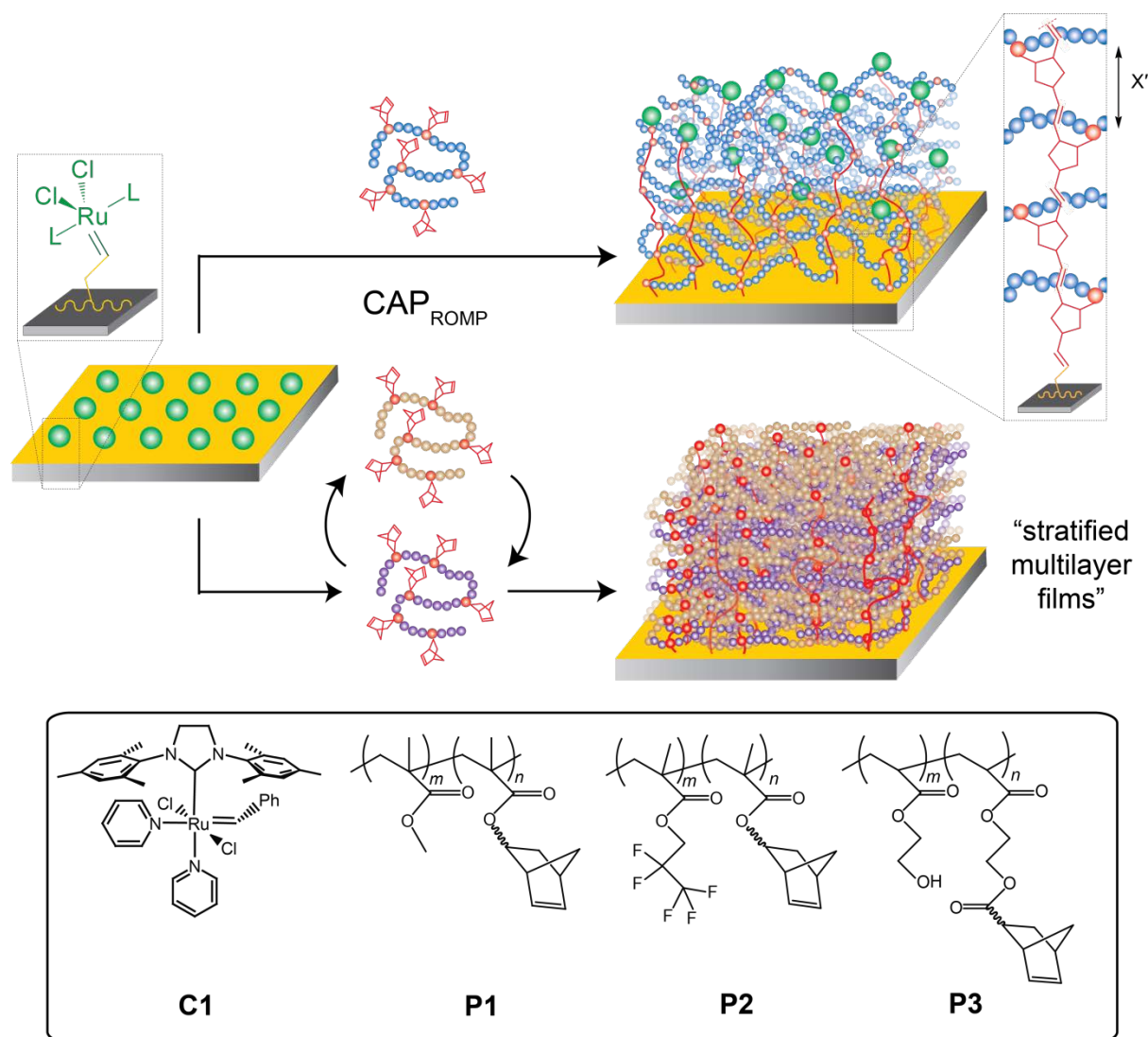
The development of advanced materials and functional coatings is an ongoing research endeavour in science and technology.^[1,2] Nanoscale coatings are particularly desirable for applications in which specific interactions or wetting characteristics are required,^[3-5] for example, self-cleaning surfaces,^[6,7] waterproof fabrics,^[5,8] microfluidic devices^[9,10] filtration systems,^[11,12] as well as advanced drug delivery devices.^[13,14] The commercial advancement of coating technologies has been realized using conventional techniques such as dip- and spray-coating.^[15-20] However, despite their ability to allow rapid deposition over large areas and their applicability to a wide variety of substrates and coating materials, fabrication of homogeneous films on complex porous or fibrous substrates is difficult to achieve as the build-up of excess coating materials may block the pores or gaps between fibres.^[21] Furthermore, these techniques can be applied effectively to surfaces with relatively large surface areas, but they are generally not applicable to micro- or nanoscale colloidal systems. In comparison, layer-by-layer (LbL) assembly^[13,14,22,23] and polymer grafting approaches^[24-26] are able to overcome this limitation, as they have been widely used to fabricate nanoscale polymer coatings on both planar and colloidal substrates. LbL assembly is a powerful technique to generate nanoscale films by the alternate deposition of complementary (bio)polymers on colloidal substrates for the fabrication of stable polymeric capsules following substrate dissolution.^[13,22,23] However, the multistep processing inherent to LbL assembly can be time-intensive. There has been a significant interest in the field of polymer grafting to modify the surface properties (e.g. wettability, dispersibility and biocompatibility)

of various substrates via both the ‘grafting-to’ and ‘grafting-from’ approaches,^[27] including recent examples on the preparation of intelligent dual-responsive surfaces from stimuli-responsive block copolymers.^[27,28] The surface properties (e.g., hydrophilicity) of such surfaces can be tuned reversibly when subjected to external stimuli, such as pH, temperature or radiation.^[27,28] It is also possible to fabricate cross-linked layered multicompositional films via the grafting-from approach by copolymerization of selective monomers and cross-linkers followed by subsequent chain extension reactions. The layer thickness extension reactions to prepare these multilayer films is dependent solely upon the end-group fidelity of the polymer brushes, which decreases with increasing polymer brush length.^[29,30] Thus, the synthesis of higher order cross-linked multilayer films with individually controlled layer properties remains a challenge.^[29-31]

Recently, we introduced a versatile approach to fabricate nanoscale films, referred to as the continuous assembly of polymers (CAP), which involves the controlled chain-growth polymerization of macrocross-linkers – (bio)macromolecules functionalized with polymerizable moieties – from initiator-functionalized substrates to afford surface-confined, cross-linked, ultrathin films with tailored properties.^[32-35] The CAP approach has distinct advantages compared to conventional dip- and spray-coating techniques, as CAP can generate nanoscale films with tunable composition and thickness (10-180 nm), controlled by reaction time, the macrocross-linker composition, and/or the type of controlled polymerization technique employed. Since the initiators are anchored to the substrate, the resulting CAP films are confined to the surface. Furthermore, the ultrathin nature of the films helps to retain the structural features of the underlying substrate, including the structure of the gaps/pores in porous substrates. The surface confinement of the CAP process also preserves the integrity of

the macrocross-linker in solution, which can be reused/recycled for subsequent CAP reactions.^[34] The recyclability of the unused macrocross-linker and mechanism of the CAP approach therefore eliminates wasteful use of excess materials caused by overdipping or overspraying, hence making the CAP process potentially economical for scale-up purposes. In addition, the CAP method can easily be implemented to prepare multilayer films. Unlike the grafting-from approach, layer thickness extension or reinitiation reactions in the CAP process do not depend exclusively on the end-group fidelity of the original chain ends, as these reactions can also occur via the ‘left-over’ polymerizable groups of the macrocross-linker deposited in the films. The versatility of the CAP technique could overcome the difficulty of the grafting approach to efficiently prepare higher order multilayer copolymer films.

In this paper, we demonstrate that the CAP_{ROMP} approach can be employed to produce versatile nanocoatings of various compositions on planar substrates (**Scheme 1**) of various compositions. Firstly, tuning the surface hydrophobicity of substrates using the CAP_{ROMP} approach is demonstrated via the fabrication of superhydrophobic coatings on various organic and inorganic materials, including cotton, cellulose, aluminium oxide, and glass. Furthermore, we demonstrate the tailored modification of cotton surfaces that exhibit switchable wettability (i.e., superhydrophobic versus superhydrophilic behavior) when subjected to iterative CAP reactions with hydrophobic and hydrophilic macrocross-linkers, thus forming multicompositional amphiphilic films in the process. To the best of our knowledge, such amphiphilic films are yet to be produced by other techniques.



Scheme 1. CAP_{ROMP} approach to tailor surface properties on planar substrates. Different surface properties were engineered using poly(methyl methacrylate) (PMMA)-based (**P1**), poly(pentafluoropropyl methacrylate) (PFPPMA)-based (**P2**), or poly(hydroxyethyl acrylate) (PHEA)-based macrocross-linker (**P3**). CAP_{ROMP} reactions were initiated by surface-bound catalyst **C1**. The polymer chain spacing is relative to the norbornene (X') repeat unit size.

2. Results and Discussion

In the CAP_{ROMP} process, the substrate surface is firstly functionalized with initiators and thereafter exposed to a solution of macrocross-linker, resulting in polymerization of the pendent norbornene groups from the surface to form cross-linked nanoscale films in a single-step. In this study, all substrates were initially functionalized with an allyl-modified poly(ethylene imine), followed by cross-metathesis with the modified 2nd generation Grubbs catalyst **C1** (1 mM in dichloromethane) to form the initiating prelayer. The macrocross-linkers (**P1-P3**), which contain between 10 to 15 mol% pendent norbornene functionalities, were employed at a concentration of 1 mM (with respect to the polymer) and selected based upon the desired characteristics of the resulting films. The following is divided into two parts that are targeted towards specifically engineering surface properties to achieve different film properties for different applications.

2.1. (Super)hydrophobic Surface Coatings

Paper technology has attracted much attention in analytical and clinical chemistry, as it has been widely used for solid-liquid separations, chromatography, and more recently as a platform for medical diagnostic devices and macroarrays.^[36] In this section, the CAP_{ROMP} approach was employed to fabricate nanoscale films on filter paper (Whatman No. 542). As a proof of concept, the assembly of poly(methyl methacrylate) (PMMA) macrocross-linker **P1** mediated by surface bound catalyst **C1** was first performed to generate hydrophobic films on filter paper. After 25 h of the CAP_{ROMP} reaction, water droplets (dyed with methylene blue) with a contact angle up to 103° were obtained (**Fig. 1a**). A kinetic experiment was performed and only a slight increase in water contact angle (measured without delay) from 98 ± 17° to 103 ± 16° was observed when the CAP reaction time was increased from 2 to 25 h (see

Supporting Information (SI), Fig. S1). However, the water absorption rates into the filter paper were found to vary significantly. The capability of the filter paper to resist water absorption increases with longer exposure times to macrocross-linker **P1** during the CAP reaction. After 2 h of the CAP reaction with **P1**, the filter paper can resist the water droplet for only 18 s before it is absorbed into the filter paper compared to 120 s for a 25 h sample (**Fig. 1b**). As we have demonstrated in our previous studies, longer CAP reaction times led to thicker films and higher surface coverage.^[32,35] Therefore, it is likely that at short reaction times (e.g. 2 h) the film coverage on the filter paper was insufficient to resist the water droplets, leading to a higher adsorption rate than the 25 h CAP_{ROMP} sample. The observed contact angle of the droplet on the **P1** coated filter paper was found to be significantly higher than the contact angle of a spin-coated **P1** film on a Si wafer ($79 \pm 7^\circ$), which is a typical contact angle for PMMA-coated surfaces.^[37,38] This difference is attributed to the higher surface roughness caused by the fibrous nature of the filter paper and the actual film assembled via CAP_{ROMP}, which as demonstrated previously, has inherent nanoscale roughness.^[32] An increase in surface roughness leads to an increase in the apparent contact angle as a result of air pockets being trapped between the water and substrate surface, which leads to a significant decrease in solid-liquid adhesion forces.^[3]

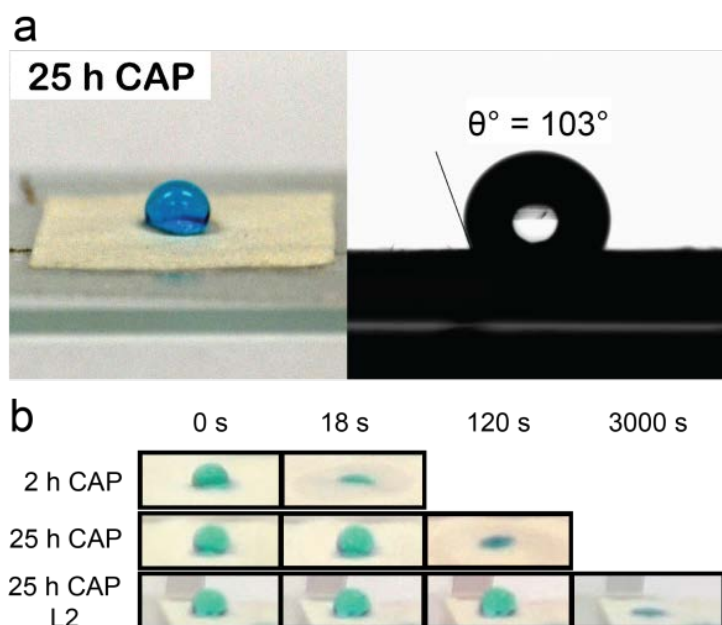


Figure 1. Wetting behaviour of filter paper coated with **P1** via CAP_{ROMP} : a) water contact angle measurement on filter paper after being subjected to 25 h of the CAP_{ROMP} reaction; and b) effect of CAP_{ROMP} polymerization time and reinitiation on the water absorption rates. L2 corresponds to layer 2 (after CAP_{ROMP} reinitiation).

Based on these observations, we expected the CAP-modified filter paper to have higher water resistivity with increasing film thickness and/or surface coverage. Therefore, to further increase the surface hydrophobicity, the CAP films were reinitiated to resume film growth and increase surface coverage.^[32] It was previously shown that the reinitiation of CAP films leads to an increase in film thickness while obtaining a more homogeneous film.^[32] The reinitiation step was performed by reimmobilizing catalyst **C1** onto the preformed films (25 h sample) by cross-metathesis reactions with any remaining allyl groups on the substrate surface and unreacted norbornenes throughout the film, followed by exposure to a **P1** solution for 25 h. After reinitiation and further film growth the water contact angle remained consistent

($105 \pm 1^\circ$), however, the coated filter paper was able to resist the water droplet until complete evaporation of the water droplet after 50 min (**Fig. 1b**). This indicates that the increase in film thickness and improvement in surface coverage resulting from reinitiation leads to an enhancement in surface hydrophobicity.

Although the surface was modified to be water resistant, the paper still exhibits the same overall physical property of an unmodified paper. The CAP-modified paper is still able to draw-up water via capillary effects when one edge of the modified filter paper was submerged in water (Fig. S2 in SI). This provides an indication that the nanocoatings were assembled onto the fibres without actually blocking the gaps between the fibres. This distinctive surface-confined property of CAP films on filter paper provides access to a broad range of applications, including antimicrobial coatings for water filtration membranes and selective coatings for paper chromatography.

Following the preliminary studies on surface modification of filter paper with the PMMA-based macrocross-linker **P1**, the versatility of the CAP approach was explored by creating superhydrophobic surfaces on substrates of various compositions. Superhydrophobic surfaces possess water contact angles greater than 150° and can be obtained by combining microstructural roughness with low surface tension chemical structures such as fluorinated compounds.^[39-42] Superhydrophobic behavior on surfaces has been an intense area of research and has attracted substantial interest from industry as a result of the wide range of potential applications, including self-cleaning surfaces and the next-generation of micro fuel cell chips.^[43-45] To demonstrate the applicability of the CAP_{ROMP} approach to fabricate such superhydrophobic surfaces, the modification of cotton substrates was initially investigated.

Waterproof woven cotton with a porous structure to allow air-flow is desirable for outdoor and sportswear since it provides greater comfort and is lightweight.^[5] The surface confined nature of the CAP approach makes it suitable for the surface modification of cotton while retaining the porous structure of the fabric. The CAP_{ROMP} procedure employed is similar to that described for the filter paper experiments and involves the initial anchoring of the catalyst initiator **C1** onto the cotton fibres, followed by exposure to the fluorinated poly(pentafluoropropylmethacrylate) (PFPPMA) macrocross-linker **P2** (pre-modified with 13 mol% of pendant norbornene groups) (**Scheme 1**). The CAP reaction was performed for 25 h, after which the modified cotton was found to exhibit superhydrophobic behavior with a contact angle of $170 \pm 2^\circ$ (**Fig. 2a,b**). In addition, the water droplet was highly stable and capable of rolling across the cotton surface without wetting it (Video S3 in SI). Notably, the superhydrophobic behavior of the surface was achieved in a single CAP reaction step without the need for subsequent film reinitiated growth. The versatility and robustness of the CAP_{ROMP} approach to fabricate superhydrophobic surfaces was demonstrated on other substrates, including glass and aluminium foil (which has a surface layer of aluminium oxide). The initial water contact angles of glass and aluminium foil prior to modification were determined to be $55 \pm 1^\circ$ and $75 \pm 2^\circ$, respectively. After CAP modification with **P2**, the water contact angles of the glass and aluminium foil were $162 \pm 2^\circ$ and $155 \pm 2^\circ$, respectively (**Fig. 2c** and **2d**, respectively). The obtained contact angle values of $> 150^\circ$ clearly confirm the successful fabrication of superhydrophobic coatings on different substrates via the CAP approach.

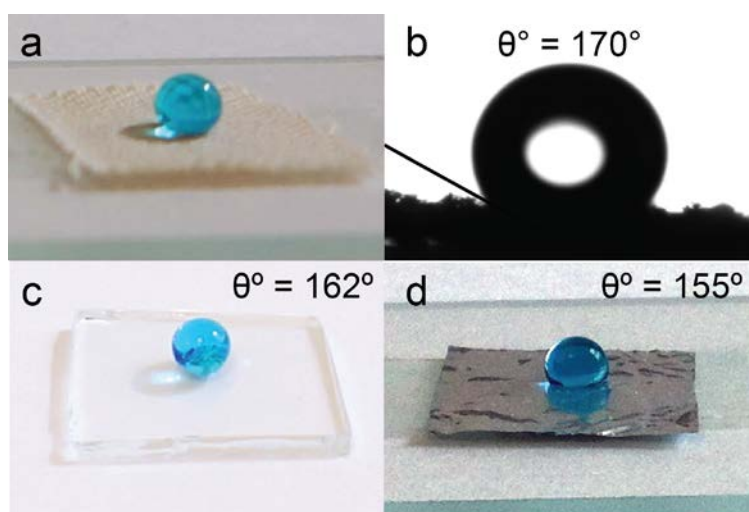


Figure 2. Superhydrophobic coatings fabricated by CAP_{ROMP} on a,b) cotton, c) glass, and d) aluminium foil.

2.2. Multilayered Amphiphilic Films

The capability of the CAP_{ROMP} approach to impart specific hydrophobicities and wetting characteristics to substrates was further investigated by the fabrication of complex layered and multicomponent films. Since CAP_{ROMP} is a rapid and controlled assembly process, and ROMP catalysts are robust and known to have high tolerance towards oxygen and moisture, it is possible to obtain multicomponent polymeric layers within a single film via iterative CAP reactions. This is demonstrated by the fabrication of amphiphilic films, whereby the CAP_{ROMP} approach was employed to reversibly switch the surface properties of cotton between superhydrophobic and superhydrophilic. Specifically, the amphiphilic film is produced by alternately exposing the previously fabricated layer to the fluorinated macrocross-linker **P2** and hydrophilic poly(2-hydroxyethyl methacrylate) (PHEA) macrocross-linker **P3** (**Fig. 3a**) without undergoing reinitiation. Initially, the cotton was modified with catalyst **C1** (as described previously) and the substrate was immersed in each polymer solution separately for

10 min, followed by washing and drying under vacuum prior to contact angle measurements. Before modification, the native cotton exhibits superhydrophilic behavior and as such does not have a contact angle as the water droplet is immediately absorbed. Following rapid exposure to **P2**, the cotton displays superhydrophobic behavior with an average water contact angle of $168 \pm 4^\circ$. This behavior can then be reversed by exposure to **P3** to recreate a superhydrophilic characteristic on cotton. This reversible switching was consistent over 11 times of alternate ‘layering’, which clearly highlights the robustness of the surface confined ROMP catalyst and the versatility of the CAP_{ROMP} approach (**Fig. 3b** and **3c**). It is worth noting that in between the CAP reaction steps, the water droplet was allowed to stand on the substrate for 30 min in an open-air environment before contact angle measurements were performed. When the outermost surface was superhydrophobic (**P2**) the water droplet was observed to be stable and there was no change in contact angle after 30 min. Conversely, when the outermost surface was superhydrophilic (**P3**) the water droplet is absorbed into the cotton, although there is a delay of 15 to 30 min depending on the number of coating steps. This is possibly attributed to the presence of hydrophobic **P2** layers in the overall multilayer films resulting in the delay in water absorption time. Nonetheless, this reversible switching of the surface properties is unique and such multilayered amphiphilic films on the nanometer scale cannot be easily prepared by other existing methods. The result also demonstrates the robustness of the CAP approach to fabricate intricate and distinctively different compositional films repeatedly without apparent loss of efficiency. It is envisaged that this novel approach towards multilayered amphiphilic films will be useful for applications involving compartmentalization of different (incompatible) components, for example, controlled release from multi-drug vehicles, and tandem catalysis. Although not shown explicitly here, the application of stimuli-responsive macrocross-linkers in CAP_{ROMP} can potentially be used to

generate a dual-responsive surface to control wetting properties, which is useful for applications such as microfluidic devices and self-cleaning surfaces.^[46]

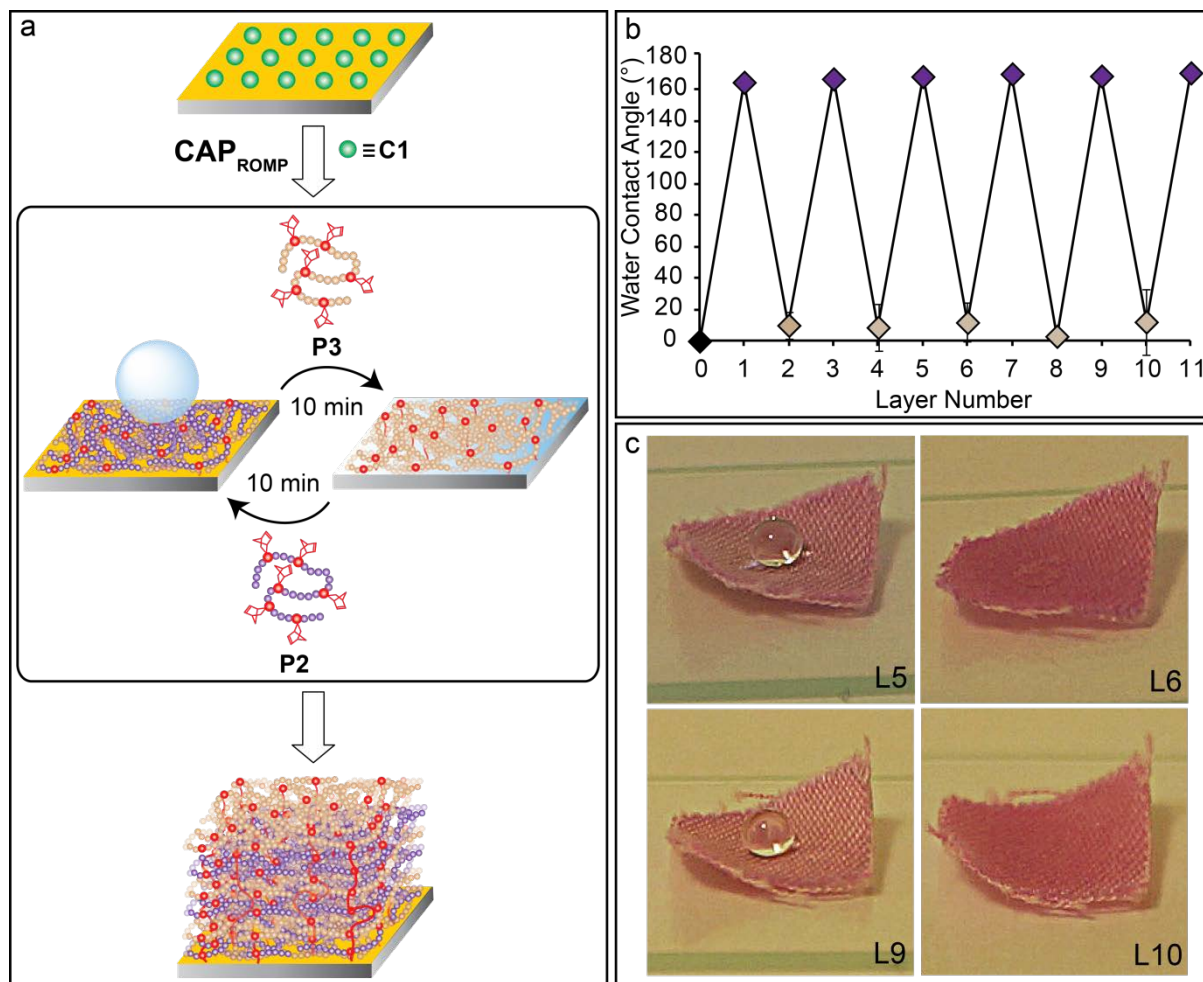


Figure 3. Fabrication of multilayered amphiphilic films via CAP_{ROMP} : a) general scheme of iterative CAP_{ROMP} reactions on cotton using macrocross-linkers **P2** and **P3**; b) contact angle measurements with respect to number of layers (odd and even layer numbers correspond to outermost coatings of **P2** and **P3**, respectively); and c) superhydrophobic and superhydrophilic behavior of the cotton after alternate layering with **P2** and **P3**. L5, L6, L9, and L10 correspond to 5, 6, 9, and 10 layers, respectively.

From the scanning electron microscopy (SEM) images of the bare and CAP-coated cotton fabrics shown in **Fig. 4a** and **4b**, it was observed that the microstructure of cotton remains unchanged. This shows that the CAP_{ROMP} technique produces a conformal coating, and again confirms that although the nanocoating was assembled onto the fibres, the gaps/holes between the bundles of fibres are retained. Upon further magnification (**Fig. 4c** and **4d**), a distinctive difference in the surface morphology was observed after the cotton was subjected to 11 iterative CAP reactions with **P2** and **P3**. SEM image of the CAP-coated fibres (**Fig. 4d**) also indicate a rough but continuous surface coverage. Such nanoscale surface roughness from these CAP_{ROMP}-generated films are expected, as demonstrated in our earlier studies with PMMA films on Si wafers.^[32,35]

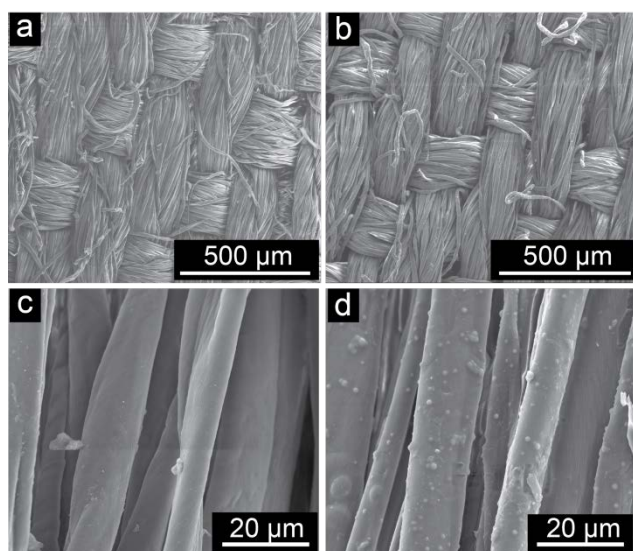


Figure 4. SEM image of a,c) the unmodified cotton fabric and b,d) the cotton coated with amphiphilic films via 11 iterative CAP reactions.

To further confirm the assembly of the amphiphilic films via the CAP_{ROMP} approach, QCM analysis was performed. In these experiments, alternate CAP_{ROMP} reactions with **P2** and **P3** were performed on gold-coated QCM electrodes under identical conditions to the reactions

conducted on cotton. **Fig. 5a** shows the percentage QCM frequency changes for the successive CAP_{ROMP} reactions after alternate exposure to macrocross-linkers **P2** and **P3** (total of 11 iterative CAP reactions). A stepwise growth was obtained after subsequent exposure to the macrocross-linkers and the change in frequency decreases with increasing ‘layering’ steps for both layer compositions. In addition, it was observed that the change in frequency after CAP_{ROMP} reactions with **P3** was more significant than those with **P2**. **Fig. 5b** shows the surface topology of a CAP-coated QCM electrode of layer 2 (**P3** film as outermost layer) and layer 11 (**P2** film as outermost layer), as analyzed by AFM, with surface roughness of 22 nm and 12 nm, respectively. Scratch AFM analysis of layer 2 and layer 11 films (in Fig. S4 in SI) reveal film thicknesses of *ca.* 50 and 150 nm, respectively. The hydrophilicity and hydrophobicity of the alternate layers, shown in **Fig. 5c**, have water contact angles of $50 \pm 2^\circ$ and $123 \pm 5^\circ$, respectively. The increase in frequency after every 10 min of CAP_{ROMP} reaction confirms the formation of stratified multicomponent films. The near asymptotic behavior of the frequency change shows a decrease in film growth efficiency with time due to the burial of the catalysts within the films, which was also observed in our earlier studies.^[32-35] It is important to note that despite the overall increase in frequency change in **Fig. 5a**, both **P2** and **P3** macrocross-linkers display distinguishable frequency changes where the more hydrophilic polymer **P3** was observed to undergo larger frequency changes compared to **P2**. The lower frequency changes associated with **P2** layers, which indicate lower mass deposition of the corresponding hydrophobic macrocross-linker, are attributed to: i) hydrophobic-hydrophilic steric repulsions between alternating hydrophilic and hydrophobic layers and/or ii) the intrinsic conformation of **P2** in dichloromethane – which is not the optimum solvent for fluorinated polymers – that led to the shielding of polymerizable norbornene groups and subsequently hindering the CAP_{ROMP} process. The decrease in surface roughness as the layer

number increases (as shown in **Fig. 5b**) is not surprising because the next generated layer fills the crevices of the prior layer. Although the formation of the **P2** layer is deduced to be thinner compared to **P3** films based on QCM measurements, stratified multicomponent films were formed nonetheless as confirmed by the alternate wetting characteristics (in **Fig. 5c**). It is noted that the water contact angle of the hydrophobic layers on the QCM electrode was observed to be lower than that on cotton due to enhanced surface roughness from the nature of rough fibres.

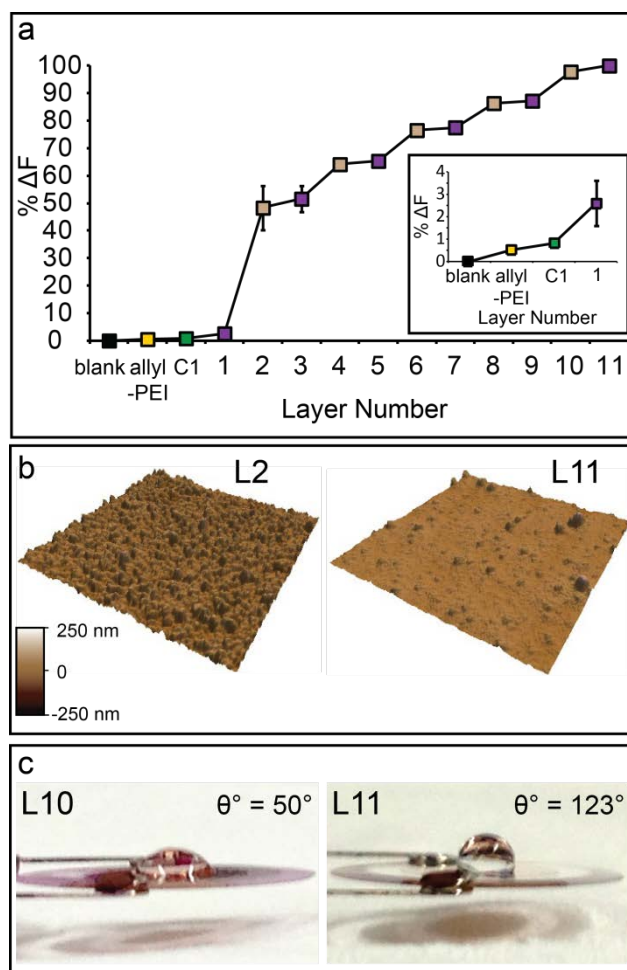


Figure 5. QCM analysis of the multilayer amphiphilic films: a) percentage QCM frequency changes due to the successive alternate CAP reactions with **P2** and **P3** on gold electrodes (inset depicts the percentage frequency changes after allyl-modified PEI deposition, catalyst

C1 immobilization and the first CAP_{ROMP} reaction with **P2** on the gold electrode). The odd layer numbers (purple) correspond to CAP reactions with hydrophobic macrocross-linker **P2**, and the even layer numbers (brown) correspond to CAP reactions with hydrophilic macrocross-linker **P3**. b) 3D height-mode AFM images of layer 2 (L2) and layer 11 (L11) on the gold electrode. c) Hydrophilicity and hydrophobicity behavior of the gold electrode after alternate layering with **P3** (represented by the 10th layer (L10) and **P2** (represented by the 11th layer (L11)).

3. Conclusions

In this study, the versatility of the CAP_{ROMP} approach to tune the surface composition and properties of nanocoatings on a wide range of substrates was demonstrated. Studies performed on filter paper using the PMMA macrocross-linker **P1** revealed that the hydrophobic behavior of the material can be manipulated by reaction time and reinitiation steps. This concept was further explored by imparting superhydrophobic behavior on various surfaces, including cotton, glass and aluminium foil using the fluorinated macrocross-linker **P2**. Subsequently, the robustness of the CAP_{ROMP} process was exploited to produce multilayered amphiphilic films containing alternate layers of the hydrophobic **P2** and hydrophilic PHEA **P3** macrocross-linkers. This alternate layering process allows for the reversible switching between hydrophobicity and hydrophilicity, as demonstrated on cotton and QCM gold-coated electrodes. From a synthetic perspective, the CAP methodology offers an efficient alternative to thin film formation strategies and as the CAP approach serves as a promising platform technology for a wide range of potential applications, including aqueous-organic filtration, next-generation textile engineering, and microelectronics. The extension of the CAP approach

to modify surface properties of particle substrates for applications including biomedical devices and drug delivery vectors will be reported in forthcoming publications.

4. Experimental

Materials: Allyl bromide (99%), 4,4'-azobis(4-cyanovaleric acid) ($\geq 75\%$), calcium hydride (CaH), *N,N'*-dicyclohexylcarbodiimide (DCC, 99%), di(ethylene glycol) vinyl ether (98%), 4-(dimethylamino)pyridine (DMAP, $\geq 99\%$), ethyl vinyl ether (EVE, 99%), 5-norbornen-2-ol (mixture of *endo* and *exo*, 99%), 5-norbornene-2-carboxylic acid (mixture of *endo* and *exo*, 98%), methacryloyl chloride (97%), and poly(ethylene imine) (PEI) ($M_w \sim 25$ kDa) were obtained from Aldrich and used without further purification. The monomers 2-hydroxyethyl acrylate (HEA, 96%) and methyl methacrylate (MMA, 99%) were obtained from Aldrich and past over plugs of inhibitor remover (Aldrich) twice to remove any inhibitors present and stored below 4 °C prior to use. *1H,1H*-Pentafluoropropyl methacrylate (PFPPMA) ($> 97\%$) was purchased from Fluorochem and used without further purification. Metathesis catalyst (IMesH₂)(Cl)₂(C₅H₅N)₂Ru=CHPh (**C1**) was prepared from the 2nd generation Grubbs catalyst (Aldrich), as described in the literature [47]. Pyridine was obtained from Scharlau and used without further purification. 2,2'-Azobis(2-methylpropionitrile) (AIBN, 98%) was obtained from Acros and used without further purification. Magnesium sulphate (MgSO₄, anhydrous), *n*-hexane, toluene, *isopropanol* and ethanol were obtained from Merck and used without further purification. Diethyl ether (DEE) and sodium hydroxide (NaOH) were obtained from Chem-Supply and used without further purification. Anhydrous *N,N*-dimethylacetamide (DMAc) was obtained by distilling from CaH *in vacuo*. Anhydrous, deoxygenated dichloromethane (DCM), and tetrahydrofuran (THF) were obtained by distillation under

argon from CaH and sodium benzophenone ketyl, respectively. Deuterated chloroform (CDCl_3), methanol (CD_3OD) and dimethylsulfoxide (d_6 -DMSO) were obtained from Cambridge Isotope Laboratories. High-purity water with a resistivity greater than $18 \text{ M}\Omega\cdot\text{cm}$ was obtained from an in-line Millipore RiOs/Origin water purification system.

Measurements: Monomer conversion was determined by GC analysis on a Shimadzu GC-17A gas chromatograph equipped with a DB-5 capillary column (Phenomenex, solid phase 5% phenylsiloxane and 95% dimethylpolysiloxane; $30 \text{ m} \times 0.25 \text{ mm} \times 0.25 \mu\text{m}$) and coupled to a GC-MS-QP5000 electron ionization mass spectrometer. Samples taken from reaction mixtures were diluted with an appropriate amount of THF and injected directly into the GC.

Polymer molecular weight characterization was carried out via GPC using a Shimadzu liquid chromatography system coupled to a Wyatt DAWN EOS MALLS detector (658 nm, 30 mW) and Wyatt OPTILAB DSP interferometric refractometer (633 nm), and using three Phenomenex Phenogel columns in series ($500, 10^4$ and 10^6 \AA porosity; $5 \mu\text{m}$ bead size) operating at $30 \text{ }^\circ\text{C}$. THF was used as the eluent at a flowrate of $1 \text{ mL}\cdot\text{min}^{-1}$. Aliquots (0.5 mL) from each reaction mixture were diluted with an appropriate amount of THF and passed through a $0.45 \mu\text{m}$ filter and injected into the GPC for analysis. Astra software (Wyatt Technology Corp.) was used to determine the molecular weight characteristics using known dn/dc values [48].

^1H and ^{13}C NMR measurements were conducted on a Varian Unity 400 MHz spectrometer at 400 and 100 MHz, respectively, using the deuterated solvent as reference and a sample concentration of *ca.* $20 \text{ mg}\cdot\text{mL}^{-1}$.

Contact angle measurements were conducted with Data Physics OCA 20 Tensiometer. Measurements were recorded with OCA software, using sessile drop profile.

The surface morphology of unmodified and CAP-coated cotton were imaged by SEM using a FEI Quanta 200 ESEM FEG. Samples were pre-coated with gold using a Dynavac Mini sputter coater prior to imaging.

Atomic force microscopy (AFM) images of air-dried CAP_{ROMP} films on QCM gold electrodes were acquired with an MFP-3D Asylum Research instrument. Typical scans were conducted in AC mode with ultrasharp SiN gold-coated cantilevers (MikroMasch, Bulgaria). Image processing and surface roughness analysis were performed using the Igor Pro software program. CAP film thicknesses were estimated by film scratching (mechanical removal) and by tracing a profile along the film and the scratched zone. The thickness measurement reported represent mean values over 3 different analysis sites per substrates.

QCM measurements were performed in an in-house-built QCM device where a frequency counter from Agilent was used to determine the film mass after each adsorption step. AT-cut quartz crystals with a fundamental resonance frequency (F_0) of 9 MHz were supplied by Kyushu Dentsu Co. (Omura-City, Nagasaki, Japan). These crystals (4.5 mm diameter) were supplied with 100 nm thick gold-coated electrodes. After CAP reactions with each alternate macrocross-linker, the crystals were removed from solution, washed thoroughly with the corresponding washing solvents, nitrogen dried, and the *in air* frequencies (F_{air}) was measured.

Synthesis of bicyclo[2.2.1]hept-5-en-2-yl methacrylate (BHEMA): This compound was prepared according to a previously published procedure [33]. ^1H NMR (400 MHz, CDCl_3 , TMS) (*endo*) δ_{H} 6.33 (*dd*, 1H, =CH), 5.97-6.00 (*m*, 2H, =CH + CHH), 5.49 (*s*, 1H, CHH), 5.31-5.34 (*m*, 1H, CHO), 3.17 (*br s*, 1H, CH), 2.85 (*br s*, 1H, CH), 2.13-2.19 (*m*, 1H, CHH), 1.88 (*s*, 3H, CH_3), 1.43-1.51 (*m*, 1H, CHH), 1.34 (*d*, 1H, CHH), 0.96 (*dt*, 1H, CHH) ppm; (*exo*) δ_{H} 6.25 (*dd*, 1H, =CH), 6.08 (*s*, 1H, CHH), 5.97-6.00 (*m*, 1H, =CH), 5.53 (*s*, 1H, CHH), 4.72-4.73 (*m*, 1H, CHO), 2.92 (*br s*, 1H, CH), 2.85 (*br s*, 1H, CH), 2.43 (*ddd*, 1H, CHH), 1.94 (*s*, 3H, CH_3), 1.67-1.74 (*m*, 1H, CHH), 1.58-1.63 (*m*, 1H, CHH), 1.43-1.51 (*m*, 1H, CHH) ppm; ^{13}C NMR (100 MHz, CDCl_3 , TMS) (*endo*) δ_{C} 167.8 (CO), 138.6 (=CH₂), 136.8 (=C(CH₃)), 131.7 (=CH), 125.2 (=CH₂), 75.5 (CHO), 47.8 (CH₂), 46.0 (CH), 42.4 (CH), 34.8 (CH₂), 18.4 (CH₃) ppm; (*exo*) δ_{C} 167.8 (CO), 141.3 (=CH), 137.0 (=C(CH₃)), 132.8 (=CH), 125.2 (=CH₂), 75.6 (CHO), 47.5 (CH₂), 46.5 (CH), 40.8 (CH), 34.9 (CH₂), 18.5 (CH₃) ppm.
 Ratio of *exo:endo* (%) = 27:73

Synthesis of norbornene functionalized PMMA macrocross-linker P1 (poly(methyl methacrylate-ran-(bicyclo[2.2.1]hept-5-en-2-yl methacrylate))): This compound was prepared according to a previously published procedure [33]. GPC-MALLS (THF): $M_w = 15.9$ kDa, $M_w/M_n = 1.8$; ^1H NMR (400 MHz, CDCl_3 , TMS) δ_{H} 6.26-6.36 (*m*, =CH), 5.99 (*br s*, =CH), 5.27 (*br s*, CHO), 4.57 (*br s*, CHO), 3.60 (*br s*, CH_3O), 3.10 (*br s*, CH), 2.88 (*br s*, CH), 2.49 (*br s*, CHH), 1.81-1.90 (*m*, CH₂), 1.43 (*br*, CH₃), 1.24-1.27 (*m*, CH₃), 1.02 (*br s*, CH₃), 0.84 (*br s*, CH₃) ppm. Pendent norbornene functionality was 7 mol% as determined by ^1H NMR spectroscopic analysis.

Synthesis of norbornene functionalized PFPMA macrocross-linker P2 (poly(pentafluoropropyl methacrylate-ran-(bicyclo[2.2.1]hept-5-en-2-yl methacrylate))): PFPMA (2 mL, 0.013 mol), BHEMA (0.23 g, 0.001 mol) and AIBN (0.043 g, 0.0003 mol) were dissolved in dioxane (8 mL). The reaction mixture was deoxygenated via bubbling of argon for 1 h and then submerged in a 100 °C oil bath for 2 h. The reaction mixture was then precipitated into pentane (80 mL) to yield polymer P3 as a white crystalline solid, 1.8 g (64 %); ¹H NMR (400 MHz, CDCl₃, TMS) δ_H 6.26-6.36 (*m*, =CH), 5.99 (*br s*, =CH), 5.27 (*br s*, CHO), 4.57 (*br s*, CHO), 4.36 (*br s*, CF₃CF₂CH₂O), 3.03 (*br s*, CH), 2.83 (*br s*, CH), 2.50 (*br s*, CHH), 1.76-2.25 (*m*, CH₂), 1.42-1.61 (*m*, CHCH₂CHO), 1.21-1.33 (*m*, CHCH₂CHO), 1.06 (*br s*, CH₃), 0.92 (*br s*, CH₃) ppm; ¹⁹F NMR (400 MHz, CDCl₃, TMS) δ_F -84.03 (*s*, CF₃), -123.30 (*s*, CF₂) ppm. Pendent norbornene functionality was 13 mol% as determined by ¹H NMR spectroscopic analysis.

Synthesis of poly((2-hydroxyethyl)acrylate) (PHEA): HEA (30.3 mmol, 3.5 g) was dissolved in EtOH (25 mL) and 4,4'-Azobis(4-cyanopentanoic acid) (0.61 mmol, 159 mg) was added. Nitrogen was bubbled through the reaction mixture for 30 min and then the mixture was heated at 60 °C for 4 h under nitrogen. The reaction was subsequently cooled in an ice bath and precipitated dropwise into DEE (200 mL) mixture. The precipitate was collected via centrifugation, redissolved in EtOH (15 mL) and the precipitation process was repeated twice before drying the product *in vacuo* to afford PHEA as a viscous polymer, 3.1 g (89 %). GPC: $M_n = 35.1$ kDa, $M_w/M_n = 1.8$. ¹H NMR (400 MHz, DMSO-*d*₆, 25 °C) δ_H 4.76 (*br*, 1H CH₂OH), 4.00 (*br*, 2H, C(=O)OCH₂), 3.55 (*br*, 2H, CH₂OH), 2.15-2.40 (*br*, 1H, CH₂CH), 1.35-1.80 (*br*, 2H, CH₂CH) ppm.

Synthesis of norbornene functionalized PHEA macrocross-linker P3 (poly((2-hydroxyethyl)acrylate-ran-(2-(5-norbornen-2-oxo)ethyl acrylate) (P(HEA-co-NOEA))): PHEA (6.8 mmol –OH, 0.79 g) was dissolved in anhydrous DMAc (10 mL) and nitrogen was bubbled through the solution for 30 min. 5-norbornene-2-carboxylic acid (0.68 mmol, 83 μ L), DCC (2 mmol, 0.42 g) and DMAP (0.2 mmol, 24.9 mg) were added. The solution was stirred at 25 °C for 7 h. Subsequently, the precipitated urea was removed by filtration and the filtrate was precipitated into DEE (100 mL). The precipitate was isolated via centrifugation, redissolved in EtOH (8 mL) and the precipitation process was repeated twice before drying the product *in vacuo* to afford **P3** as a viscous polymer, 0.2 g (26 %). GPC: $M_n = 35.2$ kDa, $M_w/M_n = 1.7$. ^1H NMR (400 MHz, DMSO- d_6 , 25 °C) δ_{H} 6.15 (*br*, 1H, **CH=C**), 5.88 (*br*, 1H, **CH=C**), 4.75 (*br*, 1H, **CH₂OH**), 4.14-4.22 (*br*, 2H **C(=O)OCH₂**), 4.00 (*br*, 2H, **C(=O)OCH₂**), 3.55 (*br*, 2H, **CH₂OH**), 2.15-2.40 (*br*, 1H, **CH₂CH**), 1.35-1.80 (*br*, 2H, **CH₂CH**) ppm. Pendant norbornene functionality was 12 mol% as determined by ^1H NMR spectroscopic analysis.

Synthesis of hyperbranched poly(N-allyl ethylene imine) (allyl-PEI): This compound was prepared according to a previously published procedure [33]. ^1H NMR (400 MHz, CD₃OD) δ_{H} 5.85 (*br s*, **CH₂=CHCH₂N**), 5.17-5.22 (*m*, **CH₂=CHCH₂N**), 3.11-3.20 (*m*, **CH₂=CHCH₂N**), 2.57 (*br s*, **N(CH₂)₂N**) ppm. Allyl functionality was 30% as determined by ^1H NMR spectroscopic analysis.

Assembly of CAP_{ROMP} films on planar substrates: All planar substrates manipulations were conducted in individual oven dried 7 mL vials under argon. Substrates (*ca.* 1 \times 1 cm) functionalized with catalyst **1** (details of this functionalization are provided in the previously

published literature [33]) were placed in vials followed by the addition of 1 mL of a 1 mM CAP-active macrocross-linker **P1** or **P2** in anhydrous and degassed dichloromethane (DCM). After standing at room temperature for a predetermined time the polymer-coated substrates were removed, washed with DCM (3×20 mL) and then exposed to 2 vol% ethyl vinyl ether (EVE) in DCM (5 mL) as a capping solution to remove the Ru catalyst from the surface of the films for 12 h before finally being washed and dried *in vacuo* prior to analysis.

Acknowledgements

The authors acknowledge the Australian Research Council under the Australian Laureate Fellowship (FF0776078, F.C.), Future Fellowship (FT110100411, G.G.Q.) and Discovery Project (DP1094147 and DP130101846, F.C., G.G.Q.) schemes for financial support of this work. Supporting Information is available online from Wiley InterScience or from the author.

Received:

Revised:

Published online:

- [1] S. F. van Dongen, H. P. de Hoog, R. J. Peters, M. Nallani, R. J. Nolte, J. C. van Hest, *Chem. Rev.* **2009**, *109*, 6212.
- [2] N. L. Rosi, C. A. Mirkin, *Chem. Rev.* **2005**, *105*, 1547.
- [3] M. Nosonovsky, B. Bhushan, *Curr. Opin. Colloid Interface Sci.* **2009**, *14*, 270.
- [4] A. Tuteja, W. Choi, M. Ma, J. M. Mabry, S. A. Mazzella, G. C. Rutledge, G. H. McKinley, R. E. Cohen, *Science* **2007**, *318*, 1618.
- [5] B. Deng, R. Cai, Y. Yu, H. Jiang, C. Wang, J. Li, L. Li, M. Yu, J. Li, L. Xie, Q. Huang, C. Fan, *Adv. Mater.* **2010**, *22*, 5473.
- [6] V. A. Ganesh, H. K. Raut, A. S. Nair, S. Ramakrishna, *J. Mater. Chem.* **2011**, *21*, 16304.
- [7] P. Roach, N. J. Shirtcliffe, M. I. Newton, *Soft Matter* **2008**, *4*, 224.
- [8] D. Cyranoski, *Nature* **2001**, *414*, 240.
- [9] T. Saitoh, A. Sekino, M. Hiraide, *Anal. Chim. Acta* **2005**, *536*, 179.
- [10] J. Yang, J. C. Chen, K. Huang, J. A. Yeh, *J. Microelectromech. Syst.* **2006**, *15*, 697.
- [11] C. R. Crick, I. P. Parkin, *Chem. Eur. J.* **2010**, *16*, 3568.
- [12] T. Sun, L. Feng, X. Gao, L. Jiang, *Acc. Chem. Res.* **2005**, *38*, 644.
- [13] J. F. Quinn, A. P. R. Johnston, G. K. Such, A. N. Zelikin, F. Caruso, *Chem. Soc. Rev.* **2007**, *36*, 707.
- [14] A. N. Zelikin, A. L. Becker, A. P. R. Johnston, K. L. Wark, F. Turatti, F. Caruso, *ACS Nano* **2007**, *1*, 63.
- [15] X. Zhang, Y. Guo, Z. Zhang, P. Zhang, *Appl. Surf. Sci.* **2012**, *258*, 7907.

- [16] H. Q. Liu, S. Szynerits, M. Pisarek, W. G. Xu, R. Boukherroub, *ACS Appl. Mater. Interfaces* **2009**, *1*, 2086.
- [17] M. H. A. Ng, L. T. Hartadi, H. Tan, C. H. P. Poa, *Nanotechnol.* **2008**, *19*, 1.
- [18] C. K. Saul, E. Burkarter, F. Thomazi, N. C. Cruz, L. S. Roman, W. H. Schreiner, *Surf. Coat. Technol.* **2007**, *202*, 194.
- [19] T. Mizukoshi, H. Matsumoto, M. Minagawa, A. Tanioka, *J. Appl. Polym. Sci.* **2007**, *103*, 3811.
- [20] I. B. Rietveld, K. Kobayashi, H. Yamada, K. Matsushige, *Soft Matter* **2009**, *5*, 593.
- [21] M. A. Aegerter, J. Puetz, G. Gasparro, N. Al-Dahoudi, *Opt. Mater.* **2004**, *26*, 155.
- [22] G. Decher, *Science* **1997**, *277*, 1232.
- [23] M. A. C. Stuart, W. T. S. Huck, J. Genzer, M. Muller, C. Ober, M. Stamm, G. B. Sukhorukoy, I. Szleifer, V. V. Tsukruk, M. Urban, *Nat. Mater.* **2010**, *9*, 110.
- [24] R. Barbey, L. Lavanant, N. Paripovic, N. Schüwer, C. Sugnaux, S. Tugulu, H. A. Klok, *Chem. Rev.*, 2009, **109**, 5437.
- [25] J. Rühle, W. J. Knoll, *J. Macromol. Sci., Polym. Rev.*, 2002, **42**, 91.
- [26] B. Zhao, W. J. Brittain, *Prog. Polym. Sci.*, 2000, **25**, 677.
- [27] J. Lindqvist, D. Nyström, E. Östmark, P. Antoni, A. Carlmark, M. Johansson, A. Hult, E. Malmström, *Biomacromolecules* **2008**, *9*, 2130.
- [28] K. Pan, X. Zhang, R. Ren, B. Cao, *J. Membrane Sci.* **2010**, *356*, 133,
- [29] A. H. Soeriyadi, C. Boyer, F. Nystrom, P. B. Zetterlund, M. R. Whittaker, *J. Am. Chem. Soc.* **2011**, *133*, 11128.
- [30] W. A. Braunecker, K. Matyjaszewski, *Prog. Polym. Sci.* **2007**, *32*, 93

- [31] Y. -Z. You, C. -Y. Hong, C. -Y. Pan, *Chem. Commun.* **2002**, 2800.
- [32] T. K. Goh, S. N. Guntari, C. J. Ochs, A. Blencowe, D. Mertz, L. A. Connal, G. K. Such, G. G. Qiao, F. Caruso, *Small* **2011**, 7, 2863.
- [33] D. Mertz, C. J. Ochs, Z. Zhu, L. Lee, S. N. Guntari, G. K. Such, T. K. Goh, L. A. Connal, A. Blencowe, G. G. Qiao, F. Caruso, *Chem. Commun.* **2011**, 47, 12601.
- [34] E. H. H. Wong, S. N. Guntari, A. Blencowe, M. P. van Koeeverden, F. Caruso, G. G. Qiao, *ACS Macro Lett.* **2012**, 1, 1020.
- [35] S. N. Guntari, T. K. Goh, A. Blencowe, E. H. H. Wong, F. Caruso, G. G. Qiao, *Polym. Chem.* **2012**, 4, 68.
- [36] A. W. Martinez, S. T. Phillips, G. M. Whitesides, *Anal. Chem.* **2010**, 82, 3.
- [37] X. Kong, T. Kawai, J. Abe, T. Iyoda, *Macromolecules* **2001**, 34, 1837.
- [38] B. Bharat, J. Y. Chae, *J. Phys. Condens. Matter.* **2008**, 20, 225010.
- [39] N. L. Abbott, J. P. Folkers, G. M. Whitesides, *Science* **1992**, 257, 1380.
- [40] H. Gau, S. Herminghaus, P. Lenz, R. Lipowsky, *Science* **1999**, 283, 46.
- [41] Y. C. Jung, B. Bhushan, *Langmuir* **2008**, 24, 6262.
- [42] C. Luo, X. L. Zuo, L. Wang, E. G. Wang, S. P. Song, J. Wang, J. Wang, C. H. Fan, Y. Cao, *Nano Lett.* **2008**, 8, 4454.
- [43] R. Fürstner, W. Barthlott, *Langmuir* **2005**, 21, 956.
- [44] A. Nakajima, K. Hashimoto, T. Watanabe, *Langmuir* **2000**, 16, 7044.
- [45] X. Zhang, F. Shi, J. Niu, Y. Jiang, Z. Wang. *J. Mater. Chem.* **2008**, 18, 621.
- [46] N. Verplanck, Y. Coffinier, V. Thomy, R. Boukherroub, *Nanoscale Res. Lett.* **2007**, 2, 577.
- [47] M. S. Sanford, J. A. Love, R. H. Grubbs, *Organometallics* **2001**, 20, 5314.

- [48] S. Michielsens, *Polymer Handbook, Vol. 2* (Eds.: J. Brandup, E. H. Immergut, E. A. Grulke), John Wiley and Sons, Hoboken **1999**, 547.

(for Table of Content use only)

The continuous assembly of polymers (CAP) is utilized as to fabricate advanced functional nanocoatings on various substrates with tunable film compositions. Its versatility is demonstrated by formation of (super)hydrophobic coating on hydrophilic substrates including paper, cotton, aluminium foil and glass. Moreover, by simple alternate dipping in hydrophilic and hydrophobic macrocross-linkers, a novel stratified amphiphilic films can be assembled via CAP.

Keywords: nanotechnology, ROMP, amphiphilic films, superhydrophobic surface

Table of Content Graphic

